Molecular Therapy
Methods & Clinical Development
Original Article

Delivery of CR2-fH Using AAV Vector Therapy as Treatment Strategy in the Mouse Model of Choroidal Neovascularization

Gloriane Schnabolk,[1] Nathaniel Parsons,[1] Elisabeth Obert,[1] Balasubramaniam Annamalai,[1] Cecile Nasarre,[1] Stephen Tomlinson,[2,3] Alfred S. Lewin,[4] and Bärbel Rohrer[1,3]

[1]Department of Ophthalmology, Medical University of South Carolina, Charleston, SC 29425, USA; [2]Department of Microbiology and Immunology, Medical University of South Carolina, Charleston, SC 29425, USA; [3]Ralph H. Johnson VA Medical Center, Division of Research, Charleston, SC 29401, USA; [4]Department of Molecular Genetics and Microbiology, University of Florida, Gainesville FL 32611, USA

Complement activation plays a significant role in age-related macular degeneration (AMD) pathogenesis, and polymorphisms interfering with factor H (fH) function, a complement alternative pathway (AP) inhibitor, are associated with increased AMD risk. We have previously validated an AP inhibitor, a fusion protein consisting of a complement receptor 2 fragment linked to the inhibitory domain of fH (CR2-fH) as an efficacious treatment for choroidal neovascularization (CNV) when delivered intravenously. Here we tested an alternative approach of AAV-mediated delivery (AAV5-VMD2-CR2-fH or AAV5-VMD2-mCherry) using subretinal delivery in C57BL/6J mice. Secretion of CR2-fH was confirmed in polarized retinal pigment epithelium (RPE) cells. A safe concentration of AAV5-VMD2-CR2-fH was identified using electroretinography, optical coherence tomography (OCT), RPE morphology, and antibody profiling. One month after gene delivery, CNV was induced using argon laser photocoagulation. OCT assessment demonstrated reduced CNV with AAV5-VMD2-CR2-fH administration. Bioavailability studies revealed that gene-therapy delivered similar levels of CR2-fH to the RPE/choroid as treatment by intravenous injections, and C3a ELISA verified reduced CNV-associated ocular C3a production. These results contribute to existing data illustrating the importance of the AP of complement in CNV development and its potential role in AMD treatment. Demonstration of AAV-vector efficacy opens new avenues for the development of treatment strategies.

INTRODUCTION

Gene therapy provides a potential alternative to the frequent invasive ocular injections received by exudative or wet age-related macular degeneration (AMD) patients. Gene therapy trials for wet AMD were triggered by the safety of adeno-associated virus (AAV) gene therapy in Leber's congenital amaurosis (reviewed by Pierce and Bennett[1]). Heier et al.[2] have reported safety and potential efficacy in a phase 1 trial using AAV2-mediated expression of soluble Flt-1, an endogenously expressed and secreted vascular endothelial growth factor (VEGF) inhibitor that binds VEGF-A2 (NCT01024998). Other clinical trials testing AAV-mediated ocular gene therapy include X-linked retinitis pigmentosa (AAV-RPGR; NCT03116113), choroideremia (AAV-REP1; NCT01461213), retinoschisis (NCT02416622), and Leber's hereditary optic neuropathy (LHON) (scAAV2-P1ND4v2; NCT02161380), and preclinical research is focusing on gene delivery in additional diseases, including Stargardt disease,[3] primary open angle glaucoma,[4] and autosomal dominant retinitis pigmentosa.[5]

Multiple complement pathway polymorphisms have been linked with an increased risk of developing AMD. These include genetic variants to complement component 3 (C3),[6] complement component 2 (C2),[7] complement component 9 (C9),[8] complement factor I (CFI),[9,10] and complement factor B (CFB).[7] However, the most frequently identified polymorphism occurs with a mutation of Y402H in complement factor H (CFH) and thereby poses the greatest single genetic risk for AMD (reviewed by Tan et al.[11]). The complement system is part of the innate and adaptive immune system, and it functions as an early response system activated at sites of injury either directly or by natural antibody binding to stress and/or injury-exposed antigens. The complement cascade triggers the production of anaphylatoxins, opsonins, and the membrane attack complex (MAC) that are involved in recruitment of immune cells, opsonization of damaged cellular material, and lysis of cells, respectively.[12] Upon activation, complement amplification by the complement alternative pathway (AP) can result in pathologically high levels of complement activation products and the generation of a pro-inflammatory micro-environment. CFH, a soluble AP inhibitor, is found abundantly in human blood[13] and can be secreted

Received 10 August 2017; accepted 6 November 2017;
https://doi.org/10.1016/j.omtm.2017.11.003.

Correspondence: Gloriane Schnabolk, Department of Ophthalmology, Medical University of South Carolina, 167 Ashley Avenue, Charleston, SC 29425, USA.
E-mail: faith@musc.edu
Correspondence: Bärbel Rohrer, Department of Ophthalmology, Medical University of South Carolina, 167 Ashley Avenue, Charleston, SC 29425, USA.
E-mail: rohrer@musc.edu

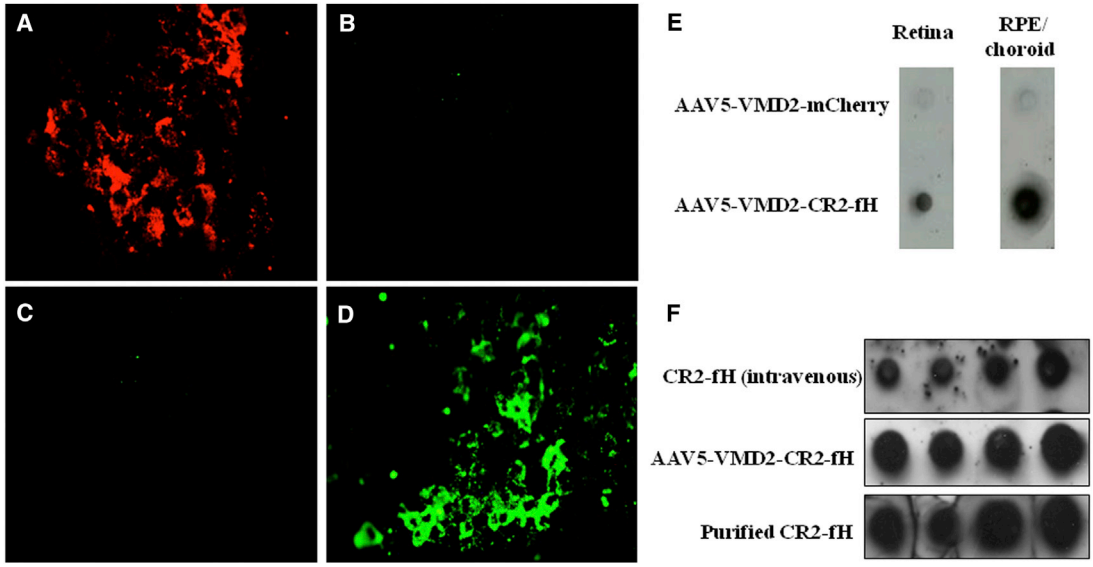

Figure 1. AAV5-Mediated Expression of CR2-fH in the Mouse RPE

(A–D) RPE/choroid sections were collected one month following subretinal injection and stained with CR2 antibody before they were flattened and mounted to glass coverslips for fluorescence microscopy. Mice injected with AAV5-VMD2-mCherry demonstrated red autofluorescence in RPE flat mounts (A), whereas mice injected with AAV5-VMD2-CR2-fH produced green CR2 immunofluorescence (D). As negative controls, mice injected with AAV-mCherry did not fluoresce when stained with CR2 (B), and mice injected with AAV5-VMD2-CR2-fH did not demonstrate red autofluorescence (C). (E) Using dot blot analysis staining for anti-CR2, CR2-fH was detected in mice injected with AAV5-VMD2-CR2-fH both in the RPE/choroid and, to a lesser extent, in the retina. (F) Bioavailability of CR2-fH in RPE/choroid was compared between intravenous injection of CR2-fH and subretinal injection of AAV5-VMD2-CR2-fH.

from various cell types, including retinal pigment epithelium (RPE) cells.[14] Because CFH plays an essential role in complement regulation,[12] mutations to this gene are expected to result in deregulation of the AP of complement activation.[15] We have pioneered the use of a site-targeted inhibitor of the AP, complement receptor 2 (CR2)-factor H (fH), in mouse models of choroidal neovascularization (CNV) and smoke-induced ocular pathology.[16,17] CR2-fH comprises a targeting domain (a fragment of CR2) and a complement inhibitory domain (short consensus repeats 1–5 for the fragment of fH). As CR2 binds iC3b, C3dg, and C3d, cell-bound opsonins that are present at sites of complement activation, the CR2 domain targets the inhibitor fH to sites of complement activation (reviewed by Holers et al.[42]). In addition, we have shown that targeting fH to sites of complement activation via CR2 significantly increases bioavailability and efficacy of fH-mediated inhibition of the AP.[18] Relevant to the studies presented here, Cashman et al.[19] have shown that a soluble form of the complement inhibitor CD59, when overexpressed via AAV2 either injected into the subretinal space (i.e., targeting RPE) or injected intravitreally (targeting Muller cells), reduced CNV in mice.

Here, we investigate the safety and efficacy of subretinal administrations of an AAV vector encoding the CR2-fH inhibitor in the mouse CNV model. We have chosen the AAV5 serotype due to its ability to infect the RPE,[20] as well as its ability to drive gene expression by 7 days post-injection.[21] RPE-selective gene expression was ensured by use of the RPE-specific VMD2 promoter.[22]

RESULTS

AAV5-Mediated CR2-fH Expression in the Mouse RPE

One month following subretinal injections of AAV5 vectors, flat mounts of RPE/choroid eyecups were either imaged for mCherry fluorescence (Figures 1A and 1C) or stained for the presence of the CR2 portion of the fusion protein (Figures 1B and 1D). As shown previously by Kong et al.[21] using an AAV5 vector driving GFP via a hybrid cytomegalovirus (CMV)-chicken β-actin promoter, RPE staining for marker genes is present 1 month after injection, with mCherry autofluorescence visible in the AAV5-VMD2-mCherry-injected eyes (Figure 1A) and CR2 immunofluorescence detectable in the RPE of AAV5-VMD2-CR2-fH-injected eyes (Figure 1D). Typically, ~60% of the RPE was transduced following subretinal injection of either vector. Corresponding dot blot analysis staining for anti-CR2 demonstrated the presence of CR2-fH in RPE/choroid and to a lesser extent in the retina of mice injected with AAV5-VMD2-CR2-fH (Figure 1E). CR2-fH was detectable in both retina and RPE/choroid fractions of injected mice, indicative of secretion into both the subretinal and the choroidal space, as suggested by cell-culture experiments of transfected RPE cells, which find secretion both apically and basally (data not shown).

To estimate whether the amount of CR2-fH present in the RPE/choroid is comparable to that obtained after tail vein injections of a therapeutic dose of protein (250 μg/animal),[16] RPE/choroid samples were probed for the presence of CR2-fH. Because CR2-fH will only bind to sites of injury, not to healthy tissue,[23] animals with

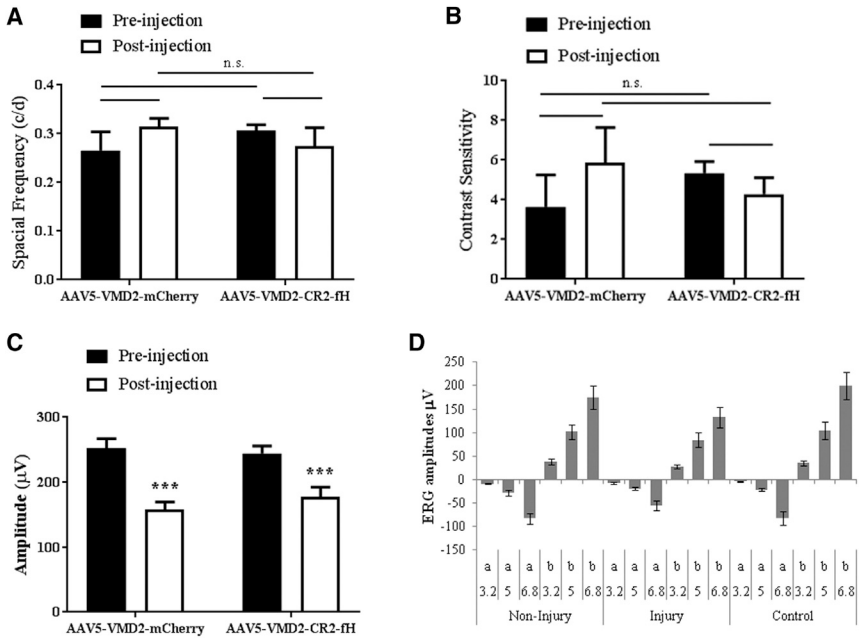

Figure 2. Vision Analysis following Subretinal AAV5-VMD2-CR2-fH Injection

(A and B) Optokinetic response was recorded before injection and one month following injection. (A) By measuring the spatial frequency threshold at a constant speed (12°/s) and contrast (100%), visual acuity was measured (n = 14–17 mice per condition). (B) To measure contrast sensitivity, the reciprocal of the contrast threshold at a fixed spatial frequency (0.131 cycles per degree) and speed (12°/s) were calculated (n = 12–18 mice per condition). (C) ERG c-wave amplitudes were measured using full-field electroretinography one month following subretinal injection (n = 12–14 mice per condition; ***$p \leq 0.001$; NS, not significant, p = 0.65). (D) Focal ERG response was recorded at 3 flash strengths for a and b waves (D). ERG analysis for areas proximal to and distal from the injection (injury) were compared to non-injected eyes (n = 10 animals per group). Data are expressed as mean ± SEM.

3-day-old CNV lesions, the time point with maximal complement activation,[16] were compared. Dot blots of the RPE/choroid extract dilution series of CNV animals treated intravenously (i.v.) with CR2-fH revealed amounts of CR2-fH comparable to those of extracts from mice injected with AAV5-VMD2-CR2-fH (Figure 1F).

Evaluation of Retinal Morphology and Function after Subretinal AAV5-VMD2-CR2-fH Injection

To monitor retinal morphology and function because of AAV5-mediated gene transfer of mCherry and CR2-fH, all mice received ophthalmic examination, including optokinetic responses (OKRs), electroretinography (ERG) (c waves and focal ERG [fERG]), and optical coherence tomography (OCT). In addition, RPE/choroid flat mounts were analyzed for RPE morphology. Lack of immunogenicity of the secretable fusion protein CR2-fH was confirmed by testing for antibody formation.

Spatial acuity and contrast sensitivity were analyzed by OKR. One month post-injection, AAV5-VMD2-CR2-mCherry and AAV5-VMD2-CR2-fH mice were determined to have no significant difference in visual acuity and contrast sensitivity (Figures 2A and 2B). The c-wave, a change in transepithelial potential of the RPE, was analyzed using full-field ERG. Significantly attenuated c-wave amplitudes were observed in both groups, consistent with damage during the needle penetration and retinal detachment, but no gene-specific effects were observed (Figure 2C). Finally, to distinguish between the effect of the local lesion and the retinal detachment of the reduction in function, fERGs were analyzed in regions proximal to and distal from the lesions in AAV5-VMD2-CR2-mCherry and AAV5-VMD2-CR2-fH mice (Figure 2D). fERG responses obtained in regions proximal to and distal from the lesion were equal in amplitudes to those elicited from control eyes without prior retinal detachment, demonstrating there is no remaining injury-related defect and no observed gene-specific effects (a-wave, p = 0.17; b-wave, p = 0.14).

The changes in the c-waves correlated with structural alteration in the RPE. RPE/choroid flat mounts were analyzed for RPE cell morphology using the cell junction marker ZO-1. In all animals, ZO-1 staining revealed a halo of unhealthy RPE cells surrounding the injection site (Figures 3A–3D). Unhealthy was defined as cells having lost their normal hexagonal shape based on eccentricity (assessing eccentricity of an ellipse) and form factor (equals 1 for a perfectly circular object) (CellProfiler software; http://www.cellprofiler.org/). Healthy mouse RPE cells from naive, non-injected, age-matched animals exhibit a form factor of ~0.79 and an eccentricity value of ~0.62. RPE cells located close to the lesion site exhibit reduced form factor and elevated eccentricity values, whereas RPE cells outside the lesion site exhibit normal values indistinguishable of those from naive animals (Figure 3E). In both groups, the lesion area covers 1.22 ± 0.12 μm^2, which based on the area of the retina being ~15.6 μm^2 (see Remtulla and Hallett[24]), represents ~8.0%. As for all other readouts, no gene-specific effects were observed. Finally, the retina beneath the healthy RPE was unaffected, as shown by OCT. The thickness of the individual layers (RPE, outer segments [OSs], inner segments [ISs], outer nuclear layer [ONL], inner nuclear layer [INL], and whole retina [WR]) were indistinguishable between animals injected with AAV5-VMD2-CR2-mCherry and those injected with AAV5-VMD2-CR2-fH (Figures 3F and 3G).

Administration of recombinant protein therapeutics can lead to the induction of anti-drug antibodies, which could interfere with the

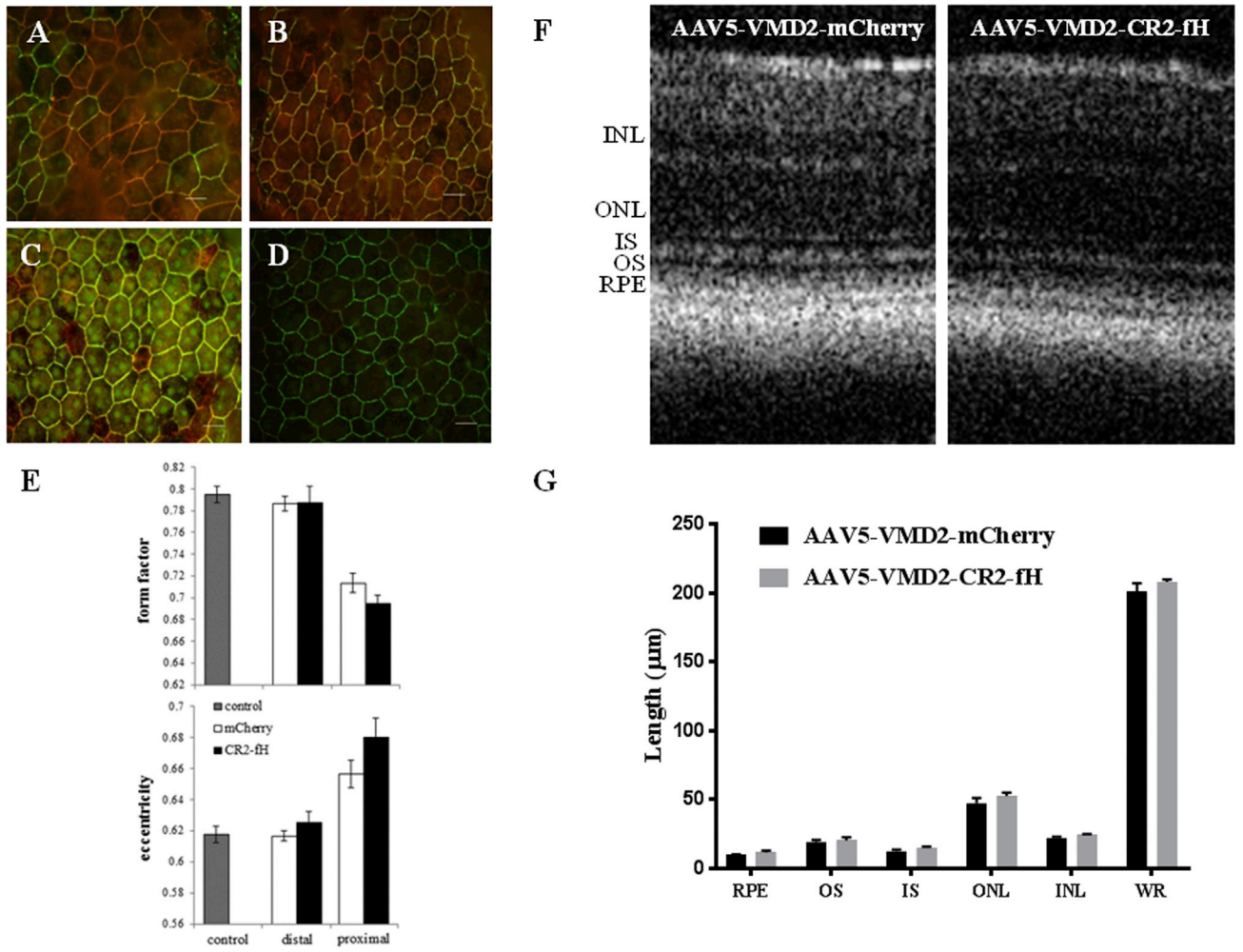

Figure 3. RPE Cell Morphology following AAV5-VMD2-CR2-fH Subretinal Injection

(A–D) RPE morphology was determined 1 month following subretinal injection using the cell junction marker ZO-1 to compare RPE cells proximal to the injection site for AAV5-VMD2-mCherry (A) and AAV5-VMD2-CR2-fH (B) and RPE cells distal from the injection site for AAV5-VMD2-mCherry (C) and AAV5-VMD2-CR2-fH (D). (E) These results were quantified using CellProfiler software to measure RPE health based on normal hexagonal shape (n = 4 animals per group). (F and G) Further analysis of the retina by OCT (F) was used to quantify the length (G) of outer segments (OS), inner segment (IS) outer nuclear layer (ONL), inner nuclear layer (INL), or whole retina (WR) length (n = 4–6 mice per condition). Data are expressed as mean ± SEM.

effect of the drug—or worse, cause tissue damage (CNV involves a natural antibody response[25]). Because CR2-fH is a secreted protein, as opposed to mCherry, which is cytoplasmic, we assessed whether mice generate antibodies against CR2-fH 1 month after the injection, even though no CR2-fH protein could be identified in mouse serum at that time point using western blotting (data not shown). No immunoglobulin G (IgG) or immunoglobulin M (IgM) antibodies recognizing CR2-fH could be detected in serum from experimental animals with AAV5-VMD2-CR2-fH or from controls with AAV5-VMD2-mCherry (Figure 4).

In summary, subretinal injections of AAV5-VMD2-CR2-mCherry or AAV5-VMD2-CR2-fH appear to be safe, with the exception of the injury induced by subretinal injections.

AAV5-VMD2-CR2-fH Reduces Complement Activation and Attenuates CNV Development

We evaluated the effectiveness of AAV5-VMD2-CR2-fH treatment on CNV lesion size 5 days following laser-induced photocoagulation. Mice were injected subretinally with either AAV5-VMD2-mCherry (control) or AAV-VMD2-CR2-fH. Mice were allowed to recover following the injection for 1 month, and subretinal reattachment was confirmed by OCT (Figures 5A–5C) and fundus photography. After reattachment (~1 month), mice underwent laser-induced CNV in all four quadrants of the eye. Using SD-OCT, we measured a significant decrease ($p \leq 0.05$) in lesion size in eyes from AAV5-VMD2-CR2-fH-treated mice (Figures 5E and 5F) compared to the control AAV5-VMD2-mCherry-treated mice (Figures 5D and 5F). This decrease of ~30% is comparable with previously published

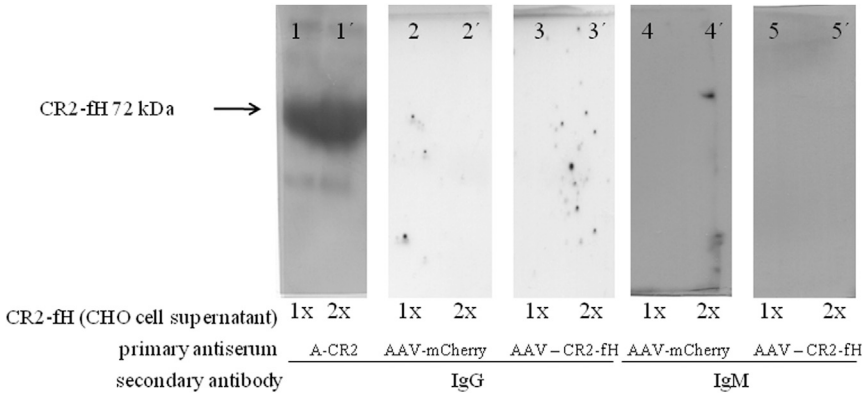

Figure 4. Subretinal AAV5 Treatment Does Not Result in Systemic Response

We examined whether mice treated with either AAV5-VMD2-mCherry or AAV5-VMD2-CR2-fH developed CR2-fH antibodies. One month following subretinal injection of AAV5-VMD2-mCherry or AAV5-VMD2-CR2-fH, sera were collected. Two concentrations of CR2-fH expressed by CHO cells (1× = 20 μL and 2× = 40 μL) were probed with sera from mice injected with either CR2-fH (panels 3, 3′, 5, and 5′) or mCherry (panels 2, 2′, 4, and 4′) as a primary antibody and with either IgG or IgM as a secondary antibody. CR2-specific antibodies were used as a positive control identifying the 72 KDa protein in control lanes (panels 1 and 1′).

results from our laboratory using CR2-fH administered via intravenous injection.[16]

To confirm that CR2-fH acts by reducing complement activation, RPE/choroid fractions collected after the OCT assessment (day 6 after the induction of CNV) were assessed for C3a, the cleavage product of C3. ELISA measurements demonstrated that CNV (4 lesions per eye) resulted in a ∼4-fold increase in C3a when compared to naive age-matched control eyes, an effect that was blocked by the presence of CR2-fH (Figure 6A). Likewise, gene expression analysis for a subset of genes (C3 to assess complement activation and Vegfa to assess angiogenesis) revealed that the changes induced by CNV (increase in C3 and Vegfa) are reversed by the expression of CR2-fH (Figure 6B). Analysis of Rpe65 demonstrated no significant change in gene expression, indicating RPE health was maintained across treated and non-treated groups.

DISCUSSION

The goal of this study was to assess the use of AAV-mediated delivery of CR2-fH as a therapeutic strategy to reduce murine CNV. The main results of the current study are as follows: (1) The CD5 signal peptide enabled CR2-fH secretion from both the apical and the basal side of the RPE when cells were transfected with the PBM-CD5-CR2-fH vector. (2) A safe concentration of AAV5-VMD2-CR2-fH was identified based on structure function testing of the retina and RPE and was defined as a concentration at which effects of the injection were due to the impact of injection, not the gene expressed. (3) An order of magnitude estimation suggests that similar amounts of CR2-fH are present in RPE/choroid samples with CNV when purified CR2-fH protein at its therapeutic dose is provided by tail vein injection compared to the expression levels produced by 3×10^8 viral genome (vg)/μL of AAV5-VMD2-CR2-fH. (4) CR2-fH expressed in the RPE was shown to reduce the development of CNV; prevent complement activation, as determined by a reduction in C3a production; and reverse CNV-associated changes in gene expression. Inhibition of CNV was observed even though only a fraction (∼60%) of the retina was detached following subretinal injection, which in previous studies is found to correlate to the amount of RPE effectively transduced.[26] This result indicates that secretion and local diffusion of CR2-fH can protect a large area of the retina, meaning that subfoveal injections may not be required for treatment of human CNV.

Complement Therapeutics in AMD

Complement inhibitors have been extensively evaluated in animal models of disease, because complement is involved in many pathological human conditions.[27] The best characterized complement inhibitors are a soluble form of CR1[28] and an anti-C5 monoclonal antibody (mAb).[29] These inhibitors act systemically, and systemic inhibition of complement is required for efficacy. Other preclinical complement inhibitors that are effective in animal models of human disease have been summarized.[27] In the mouse model of CNV, anti-complement therapeutics targeting different steps in the cascade have been found to be efficacious in reducing CNV, concomitant with a reduction in Vegfa. These complement inhibitors include small interfering RNA (siRNA) against CFB,[30] the C3 convertase inhibitor compstatin,[31] antibodies against the anaphylatoxins C3a and C5a,[32] and membrane-targeted or non-membrane-targeted soluble CD59.[33,34] Likewise, CR2-fH has been shown to reverse morphological changes in RPE and Bruch's membrane in mouse seen after continuous smoke exposure.[17] These findings, together with genome-wide association study (GWAS) and other genetic data,[35,36] suggest AP activity as the common target in wet and dry AMD. Reducing AP activation would keep the classical and lectin pathways intact, which would still allow for production of C3a and C5a, anaphylatoxins necessary for normal homeostatic processes, as well as immune response and host defense. To reduce AP activity, strategies include reducing activators (e.g., lampalizumab[37]) or increasing inhibitors (such as CFH[16]). In AMD, the most prevalent CFH variant is the Y402H polymorphism, which lies in the polyanion-binding domain of CFH (short consensus repeat [SCR] 7) and appears to impair binding of CFH to ligands, such as malondialdehyde,[38] and to BrM,[39,40] in which it would otherwise function as a membrane-bound inhibitor. In addition, we have shown that oxidative stress impairs regulation at the RPE cell surface by CFH present within the serum.[41] Hence, we have long argued that a successful strategy to supply AP inhibition would focus on generating a CFH-like molecule while relying on an alternate strategy for membrane binding, in effect providing a fH replacement therapy. We have previously shown that CR2-fH, which

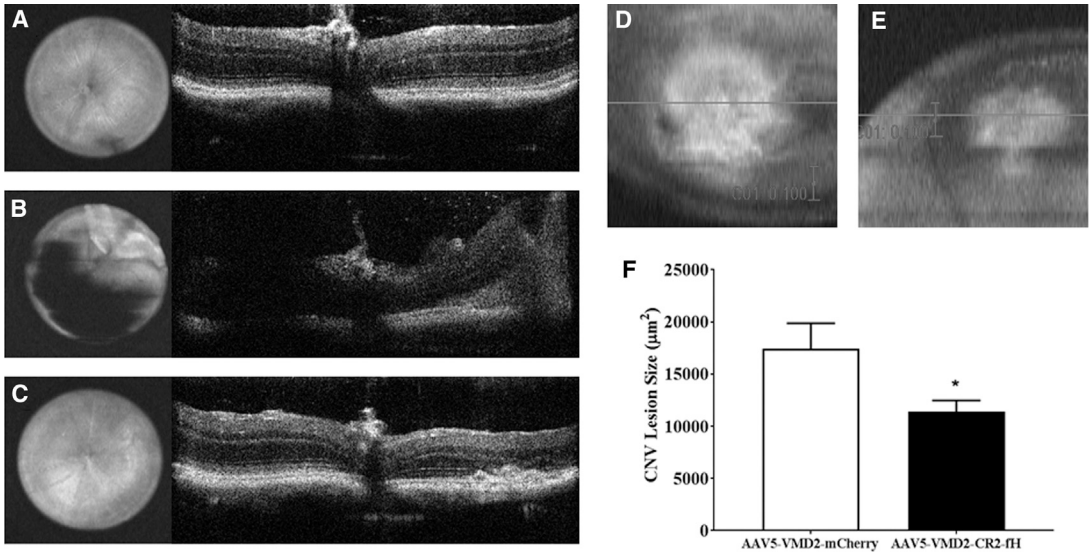

Figure 5. Subretinal Injection with AAV5-VMD2-CR2-fH Attenuates CNV

(A and B) Representative fundus and b-scan images were obtained by SD-OCT before (A) and immediately following (B) subretinal injections. (C) One month following subretinal injection of AAV5-VMD2-mCherry or AAV5-VMD2-CR2-fH, laser-induced CNV was performed and was analyzed 5 days later with SD-OCT. (D and E) *En face* fundus image of an AAV5-VMD2-mCherry-injected eye (D) and an AAV5-VMD2-CR2-fH-injected eye (E). Scale bar, 100 pixels. (F) Average CNV area. Data shown are average values (±SEM) per lesion (n = 7–8 animals per condition, $p \leq 0.05$).

relies entirely on the CR2 domain for targeting to sites of opsonin deposition, specifically targets to sites of complement activation and injury in many disease models,[23,42] including the RPE/choroid of CNV animals,[16] RPE and Bruch's membrane in smoke-induced ocular pathology,[17] and oxidatively stressed RPE cells.[25] Likewise, systemic delivery of TT30, the human therapeutic of CR2-fH, was shown to be effective in a mouse model of CNV.[43] Here we extended these findings by testing the efficacy of CR2-fH delivered by gene therapy.

Anti-complement Gene Therapy in AMD

The eye is an attractive organ for gene therapy, because it is easily accessible and immune privileged. Ever since the successful application of AAV gene therapy in Leber's congenital amaurosis (reviewed by Pierce and Bennett[1]), novel methods and application in additional diseases or disease models have been under development.[44] Relevant for our studies targeting the complement system, CD59, an inhibitor for MAC, has been shown to reduce murine CNV when provided either in the form of a soluble fusion protein or by gene therapy. CD59-IgG2a-fusion proteins injected into the vitreous or AAV2-mediated sCD59 gene expression injected either subretinally or intravitreally reduced CNV significantly.[19,33,34,45] Soluble CD59 gene expression was driven by a chicken β-actin promoter, and its ability to act as an inhibitor was confirmed by analyzing MAC deposition in the CNV lesions. Here we extended the use of gene therapy vectors to deliver complement inhibitors locally within the eye, using the AAV5 vector,[21] and ensured tissue-specific expression, using the VMD2 promoter. Efficacy for CR2-fH was noted in reducing complement activation and concomitant CNV (3×10^{11} genome copies of AAV were provided). In addition, we extended this analysis by carefully documenting the injection injury produced by subretinal injection and investigated retinal detachment. Specifically, we noted only a reduction in the RPE-driven c-wave of the full-field ERG, with corresponding changes in RPE morphology in an area around the needle injection site, whereas cone-driven OKRs (spatial acuity and contrast sensitivity), fERG in regions proximal to and distal from the injection site, and retinal structure as assessed by OCT were unaffected. No gene-specific effects were observed, indicating that the functional and structural alterations in the RPE were driven solely by the injection, not by the gene expressed. Finally, despite the secretion of CR2-fH, no generation of anti-CR2-fH IgG or IgM antibodies was detected after 1 month of protein exposure, an observation that requires confirmation at longer-term exposure.

Although our experiments documented reduction of CNV and evidence of complement inhibition with subretinal vector delivery, additional sites of delivery should be explored, because some functional and structural damage driven by the injection and retinal detachment was noted. Specifically, in future experiments, we will test intravitreal delivery, using a ubiquitous promoter and appropriate AAV serotype, to express CR2-fH in retinal ganglion cells and other cells of the inner retina. Intravitreal injection of AAV2 driving soluble Flt-1 linked to IgG1-Fc using the chicken β-actin promoter has been reported for the treatment of advanced neovascular AMD (NCT01024998).[2] Specifically, in preclinical experiments, intravitreal injections via transduction of some ganglion and transitional epithelial cells in the pars plana provided long-term expression of sFLT1. Although injections in patients were well tolerated, long-term efficacy has not yet

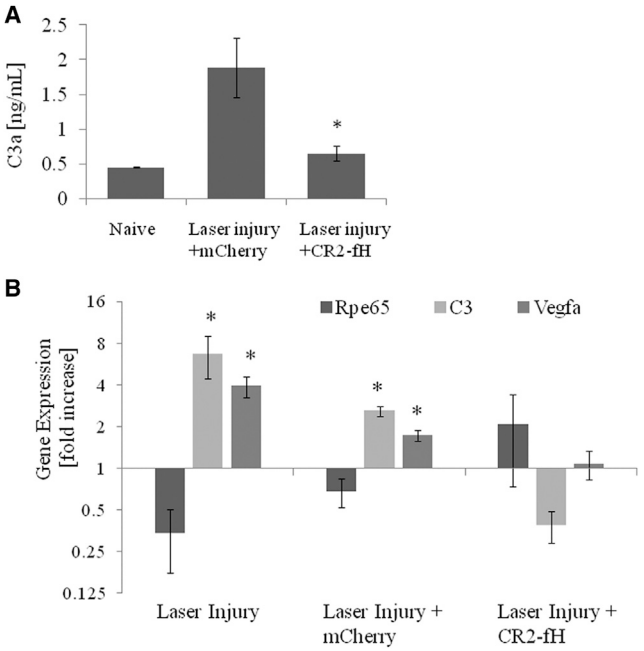

Figure 6. Gene Expression Changes in Ocular Tissues following Subretinal Injection of AAV-VMD2-CR2-fH in the Presence and Absence of Laser-Induced CNV

(A) C3a ELISA analysis for RPE/choroid fractions from naive mice compared to 6-day post-laser-induced CNV mice injected 1 month prior with either AAV-VMD2-mCherry or AAV-VMD2-CR2-fH. (B) qRT-PCR on cDNA generated from RPE/choroid fraction and retina was used to measured gene expression of Rpe65, C3, and Vegfa in 6-day post-laser-induced CNV mice injected 1 month prior with either AAV5-VMD2-mCherry or AAV5-VMD2-CR2-fH over mice with no laser-induced CNV. Data are expressed as mean ± SEM (n = 3 animals per condition performed in triplicate, $p \leq 0.05$).

been provided. It is plausible that long-term inhibition of VEGF with sFLT1 results in resistance to treatment[46] or other compensatory effects, such as an increase in complement activation.[47] These kinds of long-term compensatory effects are not expected with the CR2-fH proteins. CR2-fH has a short half-life in the circulation and only binds to sites of injury, not to healthy tissue;[23] thus, it should not interfere with complement-dependent homeostatic processes. Moreover, inhibiting the AP of complement reduces overall complement activation but retains normal levels of complement required for cellular homeostasis.[48] Finally, with the development of new viral vectors that can penetrate the inner limiting membrane,[49] a larger array of cells can presumably be targeted, providing more options for gene delivery.

In summary, we provided evidence that a targeted complement inhibitor can be used to provide effective complement inhibition in the eye, reducing AP of complement-dependent CNV progression. Demonstration of efficacy using AAV vectors opens avenues for the development of treatment strategies in AMD and other complement-dependent diseases.

MATERIALS AND METHODS

Adeno-Associated Virus Construct

The plasmid construct of CR2-fH was previously described.[16] In short, it contains the sequence encoding the 4 N-terminal SCRs of mouse CR2 (residues 1–257 of mature protein; RefSeq: M35684) followed by the 5 N-terminal SCRs of mouse fH (residues 1–303 of mature protein; RefSeq: NM009888), interspaced with a $(G_4S)_2$ linker. The expression plasmid was the previously described PBM vector with a CD5 signal peptide sequence required for secretion.[50] For confirmation purposes, the plasmid construct was transfected into ARPE-19 cells with FuGene HD transfection reagent according to the manufacturer's instructions (Roche Applied Science, Indianapolis, IN) and protein secretion into the apical and basal compartment monitored in polarized RPE cells. CR2-fH gave a single band of appropriate molecular weight by SDS-PAGE.

After confirmation of polarized secretion of CR2-fH from RPE cells (data not shown), the CR2-fH sequence was used to generate the AAV5-VMD2-CR2-fH vector (Figure S1). The same vector backbone (AAV5-VMD2) was used to generate AAV5-VMD2-mCherry.[51]

Viral Vector Injection

All animal experiments were performed in accordance with the Association for Research in Vision and Ophthalmology (ARVO) Statement for the Use of Animals in Ophthalmic and Vision Research and were approved by the University Animal Care and Use Committee. C57BL/6J mice (Jackson Laboratory, Bar Harbor, ME) were generated from a colony within Medical University of South Carolina (MUSC) to obtain mice always raised within the same microenvironment. Subretinal injections were performed using the trans-cornea route on mice 8–10 weeks of age under direct observation (dissecting microscope at 14× magnification) according to published protocols.[52,53] In short, mice were anesthetized by intraperitoneal injection (xylazine and ketamine at 20 and 80 mg/kg, respectively), their pupils were dilated (2.5% phenylephrine hydrochloric acid [HCL] and 1% atropine sulfate), and the ocular surface was anesthetized (proparacaine hydrochloride) and lubricated (2.5% hydroxypropyl methylcellulose). An aperture through the superior cornea was generated (30-1/2-gauge disposable needle), through which a 33-gauge unbeveled blunt needle mounted on a 2.5 μL Hamilton syringe (Hamilton Co., Reno, NV) was inserted to reach the subretinal space. One μL of vector suspension (in PBS) with 1% fluorescein as an indicator dye was slowly injected, with subretinal bleb formation indicating success. Retinal detachment was confirmed by OCT and fundus photography, and size and location were documented. Based on the angle of the needle required to avoid the lens, the placement of the bleb occurs in the temporal retina, with >60% of the retina becoming detached. In preliminary experiments, viral concentrations ranging from 1 μL of 1×10^{13} vg-containing particles/mL (representing a dose we found to successfully restore vision in rd12 mice[54]) to 1 μL of 1×10^{10} vg/mL were tested, comparing AAV5-VMD2-CR2-fH and AAV5-VMD2-mCherry. Expression and secretion of CR2-fH driven by 1×10^{13} vg/mL was found to reduce the ERG response 1 month after

the injection when compared to an equal concentration of AAV5-VMD2-mCherry (data not shown); a concentration of 3×10^{11} vg/mL of AAV5-VMD2-CR2-fH was found to be both efficacious and safe (see Results). Further analysis was carried out only on mice with successful retinal detachments and successful reattachments at 1 month post-injection, as confirmed by fundus photography and OCT.

CNV

Following reattachment of the retina, at around 1 month, argon laser photocoagulation (532 nm, 100 μm spot size, 0.1 s duration, 100 mW) was used to generate 4 laser spots around the optic nerve of each eye.[16] As previously described, a bubble formation at the site of the laser burn was used to determine Bruch's membrane rupture.[32] Five days following laser-induced CNV, mouse eyes were imaged by OCT and fundus photography before being sacrificed for tissue collection on day 6.

Dot Blot and Western Blot Analysis

Retina and mouse RPE/choroid were collected from CNV-lesion mice injected subretinally with AAV5-VMD2-CR2-fH, AAV5-VMD2-mCherry, or soluble CR2-fH (250 μg, via tail vein injection on day 3 after CNV induction, and collected 24 hr later). Protein was extracted by first solubilizing in radioimmunoprecipitation assay (RIPA) buffer (10 mM Tris-Hcl [pH 7.5], 300 mM NaCl, 1 mM EDTA, 1% Triton X-100, 1% SDS, and 0.1% sodium deoxycholate; Thermo Fisher Scientific, Waltham, MA) containing protease inhibitor cocktail (Sigma-Aldrich, St. Louis, MO). Whole-tissue lysates were collected following centrifugation (20,000 × *g* for 30 min at 4°C), and total protein (25 μL) was loaded directly into the wells of a 96-well plate. Using the Bio-Dot Microfiltration Apparatus (Bio-Rad Laboratories, Hercules, CA), samples were transferred onto a nitrocellulose membrane. The dotted membrane was then rinsed with Tris-buffered saline and Tween 20 (TBST) wash buffer before being blocked for 2 hr at room temperature with 5% nonfat milk in TBST buffer. CR2-fH was detected using an anti-CR2 primary antibody (10 μg/mL, rat anti-mouse CD21, clone 7G6, purified in house[50]), incubated in 5% nonfat milk/TBST (1:1,000) overnight, and visualized with a horseradish peroxidase-conjugated secondary antibody (anti-rat; Santa Cruz Biotechnology, Dallas, TX), followed by incubation with Clarity Western ECL Blotting Substrate (Bio-Rad Laboratories). For western blot analysis, supernatant from CR2-fH-expressing cultured cells was added to the Laemmli sample buffer and boiled. Samples were separated by electrophoresis on 4%–20% Criterion TGX Precast Gels (Bio-Rad Laboratories), and proteins were transferred to a polyvinylidene fluoride (PVDF) membrane. Membranes were incubated with the primary antibody against CR2 or serum (1:50) from mice treated with subretinal AAV5-VMD2-CR2-fH or AAV5-VMD2-mCherry vectors. Proteins were visualized with horseradish peroxidase-conjugated secondary antibodies (anti-mouse IgG and IgM; Santa Cruz Biotechnology), followed by incubation with Clarity Western ECL Blotting Substrate (Bio-Rad Laboratories) and chemiluminescent detection. Protein bands or dots were scanned and densities quantified using ImageJ software (Wayne Rasband, NIH, Bethesda, MD: available at https://imagej.nih.gov/ij/index.html).

Immunohistochemistry

Eyecups were collected as previously described, with the lens, anterior, and retinas removed;[16] fixed overnight with 4% paraformaldehyde (PFA); and washed in PBS. Eyecups were incubated in blocking solution (10% normal goat serum and 0.4% Triton X-100 in Tris-buffered saline) containing polyclonal ZO-1 antibody (1:200, Cat. No. 61-7300; Invitrogen) or anti-CR2 primary antibody (described earlier). Eyecups were washed following incubation with a secondary antibody (Alexa Fluor 488 goat anti-rabbit, 1:500, Cat. No. A-1008, and Alexa Fluor 488 goat anti-mouse, 1:500, Cat. No. A-11008; Invitrogen). In addition, cells were stained with Alexa Fluor 594 phalloidin (diluted in PBS 1:40, Cat. No. 12381; Invitrogen). Eyecups were then flattened onto a glass slide using four relaxing cuts, mounted with a coverslip using Fluoromount (Southern Biotechnology Associates, Birmingham, AL) and examined with fluorescence microscopy (Zeiss, Thornwood, NY) equipped with a digital black-and-white camera (Spot camera; Diagnostic Instruments, Sterling Heights, MI).

OKR Test

Visual acuity and contrast sensitivity were measured at baseline and one month following subretinal injection using OptoMotry software as previously described.[55,56] Mice were placed on an elevated pedestal placed in the center of four computer monitors displaying stimulus gratings. Following a 2 min adjustment period, OKRs were measured by observation of the mouse head response, following the direction of a rotating vertical grating, through overhead closed-circuit television (TV) cameras. Using a constant speed of 12°/s and 100% contrast, visual acuity was determined by observing the animal's response to spatial frequency display by means of a staircase procedure. By taking the reciprocal of the contrast threshold at 0.131 cycles per degree and a speed of 12°/s, contrast sensitivity between 0%–100% was determined. All tests were conducted under a mean luminance of 52 cd m^{-2}.

Full-Field and fERG

Full-field and fERG were performed at baseline and one month following subretinal injection. Mice were dark-adapted overnight and anesthetized with xylazine and ketamine (20 and 80 mg/kg, respectively), and pupils were dilated with phenylephrine HCL (2.5%) and atropine (1%). A drop of Goniovisc (Rancho Cucamonga, CA) was applied to foster the electrical contact between the electrode and the cornea. Needle electrodes inserted into the scalp and tail provided reference and ground, respectively.

Electrical responses of the RPE (c-waves) were analyzed using full-field ERG using a setup previously described.[56] In short, c-wave were recorded using a UTAS E-4000 System (LKC Technologies, Gaithersburg, MD) in response to a flash at 100 cd*s mm^{-2},[57] using corneal loop electrodes. The amplitude of the c-wave was measured from the baseline to the maximum of the peak.

fERGs were recorded using the image-guided Micron III fERG system (Phoenix Research Labs, USA) and the corneal electrodes integrated into the lens mount. A spot size of 0.5 mm was selected to measure fERGs within and away from the detached retinal area. Voltage traces

Table 1. qRT-PCR Primer Sequences

Gene Name	Symbol	Forward Primer	Reverse Primer
Retinal pigment epithelium 65	Rpe65	5′-TTCTGAGTGTGGTGGTGAGC-3′	5′-AGTCCATGGAAGGTCACAGG-3′
Complement component 3	C3	5′-TCAGATAAGGAGGGGCACAA-3′	5′-ATGAAGAGGTACCCACTCTGGA-3′
Vascular endothelial growth factor A	Vegfa	5′-AGCACAGCAGATGTGAATGC-3′	5′-TTTCTTGCGCTTTCGTTTTT-3′
Actin, β	Actb	5′-AGCTGAGAGGGAAATCGTGC-3′	5′-ACCAGACAGCACTGTGTTG-3′

were recorded in response to three flash strengths (3.2, 5, and 6.8 cd m^2) at a duration of 2 ms, and analyzed with LabScribe software (v.3.015200) that comes standard with the fERG system. Ten sweeps were averaged for the low flash strength, and 5 sweeps were averaged for the higher flash strengths; however, outlier sweeps, in which the software could not properly identify the trough of the a-wave or the peak of the b-wave, were manually excluded from the calculations.

RPE Morphology Assessment

The CellProfiler v.2.11 software (http://www.cellprofiler.org/) was used to evaluate RPE morphology as previously described.[58] TIF files of images of equal size and exposure time were first imported into the software and analyzed using a customizable script. Cells were compared using the pipeline neighboring cells from which the form factor (in which a perfectly circular object equals 1) and eccentricity (the degree, measured between 0 and 1, to which an object represents an ellipse) were obtained. Morphology of RPE cells was analyzed within the peri-lesion area of the injection site and compared to the tiling pattern of an area (45 × 74 μm, depth by width) surrounding the peri-lesion. Morphology measurements for age-matched, untreated C57BL/6J mice were obtained for reference purposes.

OCT

OCT was used to quantify retinal thickness[56] and analyze CNV lesion size on day 5 after laser treatment as previously described.[59–61] Mice were anesthetized before imaging, and eyes were kept hydrated with normal saline. Using an SD-OCT Bioptigen Spectral Domain Ophthalmic Imaging System (Bioptigen, Durham NC), the eyes were imaged.

To assess retina structure, rectangular volume scans were taken in the nasal quadrant from the optic disc, each volume consisting of 33 B scans (1,000 A scans per B scan). Five separate scans were collected and averaged to generate a high-resolution image. Vertical calipers were placed to measure the thickness of the different retinal layers for each scan. All measurements were taken 500 μm from the optic disc.[56]

For CNV lesion analyses, rectangular volume scans images set at 1.6 × 1.6 mm, consisting of 100 B scans (1,000 A scans per B scan) were acquired. Using methods previously described by Giani et al.,[62] the cross-sectional area of the lesion was measured by using the *en face* fundus reconstruction tool to ascertain the midline passing through the RPE and Bruch's membrane rupture, with the axial interval positioned at the level of the RPE/choroid complex. ImageJ software was used to measure the area around the hyporeflective spot produced on the fundus image, with vertical calipers set at 0.1 mm at the site of each lesion. Based on the size of the individual pixels (1.6 × 1.6 μm), the lesion sizes were calculated.

C3a ELISA

C3a levels were measured in RPE/choroid/sclera (referred to as RPE/choroid) fractions of mice treated by subretinal injection with either AAV5-VMD2-mCherry or AAV5-VMD2-CR2-fH before CNV, as well as control eyes using Mouse Complement C3a ELISA from LifeSpan Biosciences (Seattle, WA). RPE/choroid tissues were quickly prepared on ice by rinsing with ice-cold PBS to remove excess blood. Cells were then lysed by ultrasonication using ice-cold PBS. Centrifugation of the final homogenate was performed at 5,000 × *g* for 5 min before continuing with the assay procedure as described in the manufacturer's protocol. Final values were read using a microplate reader set at 450 nm.

qRT-PCR

Retina and RPE/choroid fractions of the mouse eye were isolated on day 6 following laser-induced photocoagulation and stored at −80°C until use. Using the miRNeasy Kit (QIAGEN, Valencia, CA), total RNA was isolated and purified, and RNA with a 260:280 ratio of 1.95–2.1 (Take 3 Micro-Volume Plates, Biotek, Winooski, VT) was used to generate first-strand cDNA (QIAGEN). PCR amplifications were performed in triplicate as previously described[56] using the Realplex 2 Mastercycler (Eppendorf, Hauppauge, NY). Primer sequences for each gene product are listed in Table 1. Cycle number (Ct value) was used to obtain quantitative values as previously described,[63] with genes of interest normalized to β-actin. Using the *Z* test, fold differences between AAV5-VMD2-fH and AAV5-mCherry in the presence or absence of CNV (control) were determined.

Statistics

Data are presented as mean ± SEM. Single comparisons were analyzed using unpaired t tests, with mean value differences considered significant at $p \leq 0.05$. Fold changes in qRT-PCR experiments were analyzed by *Z* test ($p < 0.05$). For data consisting of multiple groups and repeated measures, repeated-measure ANOVA was used.

SUPPLEMENTAL INFORMATION

Supplemental Information includes one figure and can be found with this article online at https://doi.org/10.1016/j.omtm.2017.11.003.

AUTHOR CONTRIBUTIONS

Conceptualization, G.S. and B.R.; Methodology, G.S., N.P., and A.S.L., Investigation, G.S., N.P., E.O., B.A., and C.N.; Writing – Original Draft, G.S. and B.R.; Writing – Review and Editing, G.S., B.R., A.S.L., and S.T.; Funding Acquisition, B.R., A.S.L., and S.T.; Resources, B.R., A.S.L., and S.T.

CONFLICTS OF INTEREST

S.T. and B.R. are patent holders for the use of CR2-fH in complement-dependent diseases. This patent is licensed to Alexion Therapeutics. A.S.L. acts as a consultant for the Astellas Institute for Regenerative Medicine. All other authors have no financial conflicts of interest.

ACKNOWLEDGMENTS

Funding for this project was provided in part by the Department of Veterans Affairs merit awards RX000444 (to B.R.) and 1I01RX001141 and 1I21RX002363 (to S.T.) and the NIH R01 EY019320 and R01 EY024581 (to B.R.), R01 EY026268 and P30 EY02172 (A.S.L.), and R01 DK102912 (S.T.). Animal studies were conducted in a facility constructed with support from the NIH (C06 RR015455).

REFERENCES

1. Pierce, E.A., and Bennett, J. (2015). The status of RPE65 gene therapy trials: safety and efficacy. Cold Spring Harb. Perspect. Med. *5*, a017285.
2. Heier, J.S., Kherani, S., Desai, S., Dugel, P., Kaushal, S., Cheng, S.H., Delacono, C., Purvis, A., Richards, S., Le-Halpere, A., et al. (2017). Intravitreous injection of AAV2-sFLT01 in patients with advanced neovascular age-related macular degeneration: a phase 1, open-label trial. Lancet *390*, 50–61.
3. Han, Z., Conley, S.M., Makkia, R.S., Cooper, M.J., and Naash, M.I. (2012). DNA nanoparticle-mediated ABCA4 delivery rescues Stargardt dystrophy in mice. J. Clin. Invest. *122*, 3221–3226.
4. Li, M., Xu, J., Chen, X., and Sun, X. (2009). RNA interference as a gene silencing therapy for mutant MYOC protein in primary open angle glaucoma. Diagn. Pathol. *4*, 46.
5. Rex, T.S., Kasmala, L., Bond, W.S., de Lucas Cerrillo, A.M., Wynn, K., and Lewin, A.S. (2016). Erythropoietin slows photoreceptor cell death in a mouse model of autosomal dominant retinitis pigmentosa. PLoS ONE *11*, e0157411.
6. Yates, J.R., Sepp, T., Matharu, B.K., Khan, J.C., Thurlby, D.A., Shahid, H., Clayton, D.G., Hayward, C., Morgan, J., Wright, A.F., et al.; Genetic Factors in AMD Study Group (2007). Complement C3 variant and the risk of age-related macular degeneration. N. Engl. J. Med. *357*, 553–561.
7. Gold, B., Merriam, J.E., Zernant, J., Hancox, L.S., Taiber, A.J., Gehrs, K., Cramer, K., Neel, J., Bergeron, J., Barile, G.R., et al.; AMD Genetics Clinical Study Group (2006). Variation in factor B (BF) and complement component 2 (C2) genes is associated with age-related macular degeneration. Nat. Genet. *38*, 458–462.
8. Seddon, J.M., Yu, Y., Miller, E.C., Reynolds, R., Tan, P.L., Gowrisankar, S., Goldstein, J.I., Triebwasser, M., Anderson, H.E., Zerbib, J., et al. (2013). Rare variants in CFI, C3 and C9 are associated with high risk of advanced age-related macular degeneration. Nat. Genet. *45*, 1366–1370.
9. Fagerness, J.A., Maller, J.B., Neale, B.M., Reynolds, R.C., Daly, M.J., and Seddon, J.M. (2009). Variation near complement factor I is associated with risk of advanced AMD. Eur. J. Hum. Genet. *17*, 100–104.
10. Fritsche, L.G., Igl, W., Bailey, J.N., Grassmann, F., Sengupta, S., Bragg-Gresham, J.L., Burdon, K.P., Hebbring, S.J., Wen, C., Gorski, M., et al. (2016). A large genome-wide association study of age-related macular degeneration highlights contributions of rare and common variants. Nat. Genet. *48*, 134–143.
11. Tan, P.L., Bowes Rickman, C., and Katsanis, N. (2016). AMD and the alternative complement pathway: genetics and functional implications. Hum. Genomics *10*, 23.
12. Müller-Eberhard, H.J. (1988). Molecular organization and function of the complement system. Annu. Rev. Biochem. *57*, 321–347.
13. Pangburn, M.K., Rawal, N., Cortes, C., Alam, M.N., Ferreira, V.P., and Atkinson, M.A. (2009). Polyanion-induced self-association of complement factor H. J. Immunol. *182*, 1061–1068.
14. Kim, Y.H., He, S., Kase, S., Kitamura, M., Ryan, S.J., and Hinton, D.R. (2009). Regulated secretion of complement factor H by RPE and its role in RPE migration. Graefes Arch. Clin. Exp. Ophthalmol *247*, 651–659.
15. Rodriguez, E., Rallapalli, P.M., Osborne, A.J., and Perkins, S.J. (2014). New functional and structural insights from updated mutational databases for complement factor H, factor I, membrane cofactor protein and C3. Biosci. Rep. *34*, e00146.
16. Rohrer, B., Long, Q., Coughlin, B., Wilson, R.B., Huang, Y., Qiao, F., Tang, P.H., Kunchithapautham, K., Gilkeson, G.S., and Tomlinson, S. (2009). A targeted inhibitor of the alternative complement pathway reduces angiogenesis in a mouse model of age-related macular degeneration. Invest. Ophthalmol. Vis. Sci. *50*, 3056–3064.
17. Woodell, A., Jones, B.W., Williamson, T., Schnabolk, G., Tomlinson, S., Atkinson, C., and Rohrer, B. (2016). A targeted inhibitor of the alternative complement pathway accelerates recovery from smoke-induced ocular injury. Invest. Ophthalmol. Vis. Sci. *57*, 1728–1737.
18. Huang, Y., Qiao, F., Atkinson, C., Holers, V.M., and Tomlinson, S. (2008). A novel targeted inhibitor of the alternative pathway of complement and its therapeutic application in ischemia/reperfusion injury. J. Immunol *181*, 8068–8076.
19. Cashman, S.M., Gracias, J., Adhi, M., and Kumar-Singh, R. (2015). Adenovirus-mediated delivery of factor H attenuates complement C3 induced pathology in the murine retina: a potential gene therapy for age-related macular degeneration. J. Gene Med. *17*, 229–243.
20. Pang, J.J., Lauramore, A., Deng, W.T., Li, Q., Doyle, T.J., Chiodo, V., Li, J., and Hauswirth, W.W. (2008). Comparative analysis of in vivo and in vitro AAV vector transduction in the neonatal mouse retina: effects of serotype and site of administration. Vision Res. *48*, 377–385.
21. Kong, F., Li, W., Li, X., Zheng, Q., Dai, X., Zhou, X., Boye, S.L., Hauswirth, W.W., Qu, J., and Pang, J.J. (2010). Self-complementary AAV5 vector facilitates quicker transgene expression in photoreceptor and retinal pigment epithelial cells of normal mouse. Exp. Eye Res. *90*, 546–554.
22. Esumi, N., Oshima, Y., Li, Y., Campochiaro, P.A., and Zack, D.J. (2004). Analysis of the VMD2 promoter and implication of E-box binding factors in its regulation. J. Biol. Chem. *279*, 19064–19073.
23. Alawieh, A., and Tomlinson, S. (2016). Injury site-specific targeting of complement inhibitors for treating stroke. Immunol. Rev. *274*, 270–280.
24. Remtulla, S., and Hallett, P.E. (1985). A schematic eye for the mouse, and comparisons with the rat. Vision Res. *25*, 21–31.
25. Joseph, K., Kulik, L., Coughlin, B., Kunchithapautham, K., Bandyopadhyay, M., Thiel, S., Thielens, N.M., Holers, V.M., and Rohrer, B. (2013). Oxidative stress sensitizes retinal pigmented epithelial (RPE) cells to complement-mediated injury in a natural antibody-, lectin pathway- and phospholipid epitope-dependent manner. J. Biol. Chem. *288*, 12753–12765.
26. Du, W., Tao, Y., Deng, W.T., Zhu, P., Li, J., Dai, X., Zhang, Y., Shi, W., Liu, X., Chiodo, V.A., et al. (2015). Vitreal delivery of AAV vectored Cnga3 restores cone function in CNGA3−/−/Nrl−/− mice, an all-cone model of CNGA3 achromatopsia. Hum. Mol. Genet. *24*, 3699–3707.
27. Ricklin, D., and Lambris, J.D. (2007). Complement-targeted therapeutics. Nat. Biotechnol. *25*, 1265–1275.
28. Whiss, P.A. (2002). Pexelizumab Alexion. Curr. Opin. Investig. Drugs *3*, 870–877.
29. Kaplan, M. (2002). Eculizumab (Alexion). Curr. Opin. Investig. Drugs *3*, 1017–1023.
30. Bora, N.S., Kaliappan, S., Jha, P., Xu, Q., Sohn, J.H., Dhaulakhandi, D.B., Kaplan, H.J., and Bora, P.S. (2006). Complement activation via alternative pathway is critical in the development of laser-induced choroidal neovascularization: role of factor B and factor H. J. Immunol. *177*, 1872–1878.
31. Sun, Y., Yu, W., Huang, L., Hou, J., Gong, P., Zheng, Y., Zhao, M., Zhou, P., and Li, X. (2012). Is asthma related to choroidal neovascularization? PLoS ONE *7*, e35415.
32. Nozaki, M., Raisler, B.J., Sakurai, E., Sarma, J.V., Barnum, S.R., Lambris, J.D., Chen, Y., Zhang, K., Ambati, B.K., Baffi, J.Z., and Ambati, J. (2006). Drusen complement

components C3a and C5a promote choroidal neovascularization. Proc. Natl. Acad. Sci. USA *103*, 2328–2333.

33. Bora, N.S., Jha, P., Lyzogubov, V.V., Kaliappan, S., Liu, J., Tytarenko, R.G., Fraser, D.A., Morgan, B.P., and Bora, P.S. (2010). Recombinant membrane-targeted form of CD59 inhibits the growth of choroidal neovascular complex in mice. J. Biol. Chem. *285*, 33826–33833.

34. Cashman, S.M., Ramo, K., and Kumar-Singh, R. (2011). A non membrane-targeted human soluble CD59 attenuates choroidal neovascularization in a model of age related macular degeneration. PLoS ONE *6*, e19078.

35. Cooke Bailey, J.N., Pericak-Vance, M.A., and Haines, J.L. (2014). Genome-wide association studies: getting to pathogenesis, the role of inflammation/complement in age-related macular degeneration. Cold Spring Harb. Perspect. Med. *4*, a017186.

36. Black, J.R., and Clark, S.J. (2016). Age-related macular degeneration: genome-wide association studies to translation. Genet. Med *18*, 283–289.

37. Wright, C.B., and Ambati, J. (2017). Dry age-related macular degeneration pharmacology. Handb. Exp. Pharmacol. *242*, 321–336.

38. Weismann, D., Hartvigsen, K., Lauer, N., Bennett, K.L., Scholl, H.P., Charbel Issa, P., Cano, M., Brandstätter, H., Tsimikas, S., Skerka, C., et al. (2011). Complement factor H binds malondialdehyde epitopes and protects from oxidative stress. Nature *478*, 76–81.

39. Clark, S.J., Higman, V.A., Mulloy, B., Perkins, S.J., Lea, S.M., Sim, R.B., and Day, A.J. (2006). His-384 allotypic variant of factor H associated with age-related macular degeneration has different heparin binding properties from the non-disease-associated form. J. Biol. Chem. *281*, 24713–24720.

40. Clark, S.J., Perveen, R., Hakobyan, S., Morgan, B.P., Sim, R.B., Bishop, P.N., and Day, A.J. (2010). Impaired binding of the age-related macular degeneration-associated complement factor H 402H allotype to Bruch's membrane in human retina. J. Biol. Chem. *285*, 30192–30202.

41. Thurman, J.M., Renner, B., Kunchithapautham, K., Ferreira, V.P., Pangburn, M.K., Ablonczy, Z., Tomlinson, S., Holers, V.M., and Rohrer, B. (2009). Oxidative stress renders retinal pigment epithelial cells susceptible to complement-mediated injury. J. Biol. Chem. *284*, 16939–16947.

42. Holers, V.M., Rohrer, B., and Tomlinson, S. (2013). CR2-mediated targeting of complement inhibitors: bench-to-bedside using a novel strategy for site-specific complement modulation. Adv. Exp. Med. Biol. *735*, 137–154.

43. Rohrer, B., Coughlin, B., Bandyopadhyay, M., and Holers, V.M. (2012). Systemic human CR2-targeted complement alternative pathway inhibitor ameliorates mouse laser-induced choroidal neovascularization. J. Ocul. Pharmacol. Ther *28*, 402–409.

44. Liu, M.M., Tuo, J., and Chan, C.C. (2011). Republished review: gene therapy for ocular diseases. Postgrad. Med. J. *87*, 487–495.

45. Adhi, M., Cashman, S.M., and Kumar-Singh, R. (2013). Adeno-associated virus mediated delivery of a non-membrane targeted human soluble CD59 attenuates some aspects of diabetic retinopathy in mice. PLoS ONE *8*, e79661.

46. Yang, S., Zhao, J., and Sun, X. (2016). Resistance to anti-VEGF therapy in neovascular age-related macular degeneration: a comprehensive review. Drug Des. Devel. Ther. *10*, 1857–1867.

47. Keir, L.S., Firth, R., Aponik, L., Feitelberg, D., Sakimoto, S., Aguilar, E., Welsh, G.I., Richards, A., Usui, Y., Satchell, S.C., et al. (2017). VEGF regulates local inhibitory complement proteins in the eye and kidney. J. Clin. Invest. *127*, 199–214.

48. Alawieh, A., Elvington, A., Zhu, H., Yu, J., Kindy, M.S., Atkinson, C., and Tomlinson, S. (2015). Modulation of post-stroke degenerative and regenerative processes and subacute protection by site-targeted inhibition of the alternative pathway of complement. J. Neuroinflammation *12*, 247.

49. Boyd, R.F., Sledge, D.G., Boye, S.L., Boye, S.E., Hauswirth, W.W., Komáromy, A.M., Petersen-Jones, S.M., and Bartoe, J.T. (2016). Photoreceptor-targeted gene delivery using intravitreally administered AAV vectors in dogs. Gene Ther. *23*, 223–230.

50. Song, H., He, C., Knaak, C., Guthridge, J.M., Holers, V.M., and Tomlinson, S. (2003). Complement receptor 2-mediated targeting of complement inhibitors to sites of complement activation. J. Clin. Invest. *111*, 1875–1885.

51. Ryals, R.C., Boye, S.L., Dinculescu, A., Hauswirth, W.W., and Boye, S.E. (2011). Quantifying transduction efficiencies of unmodified and tyrosine capsid mutant AAV vectors in vitro using two ocular cell lines. Mol. Vis. *17*, 1090–1102.

52. Pang, J.J., Boye, S.L., Kumar, A., Dinculescu, A., Deng, W., Li, J., Li, Q., Rani, A., Foster, T.C., Chang, B., et al. (2008). AAV-mediated gene therapy for retinal degeneration in the rd10 mouse containing a recessive PDEbeta mutation. Invest. Ophthalmol. Vis. Sci. *49*, 4278–4283.

53. Pang, J., Boye, S.E., Lei, B., Boye, S.L., Everhart, D., Ryals, R., Umino, Y., Rohrer, B., Alexander, J., Li, J., et al. (2010). Self-complementary AAV-mediated gene therapy restores cone function and prevents cone degeneration in two models of Rpe65 deficiency. Gene Ther. *17*, 815–826.

54. Pang, J.J., Chang, B., Hawes, N.L., Hurd, R.E., Davisson, M.T., Li, J., Noorwez, S.M., Malhotra, R., McDowell, J.H., Kaushal, S., et al. (2005). Retinal degeneration 12 (rd12): a new, spontaneously arising mouse model for human Leber congenital amaurosis (LCA). Mol. Vis. *11*, 152–162.

55. Prusky, G.T., Alam, N.M., Beekman, S., and Douglas, R.M. (2004). Rapid quantification of adult and developing mouse spatial vision using a virtual optomotor system. Invest. Ophthalmol. Vis. Sci. *45*, 4611–4616.

56. Woodell, A., Coughlin, B., Kunchithapautham, K., Casey, S., Williamson, T., Ferrell, W.D., Atkinson, C., Jones, B.W., and Rohrer, B. (2013). Alternative complement pathway deficiency ameliorates chronic smoke-induced functional and morphological ocular injury. PLoS ONE *8*, e67894.

57. Ablonczy, Z., Dahrouj, M., and Marneros, A.G. (2014). Progressive dysfunction of the retinal pigment epithelium and retina due to increased VEGF-A levels. FASEB J. *28*, 2369–2379.

58. Obert, E., Strauss, R., Brandon, C., Grek, C., Ghatnekar, G., Gourdie, R., and Rohrer, B. (2017). Targeting the tight junction protein, zonula occludens-1, with the connexin43 mimetic peptide, αCT1, reduces VEGF-dependent RPE pathophysiology. J. Mol. Med. (Berl.) *95*, 535–552.

59. Schnabolk, G., Coughlin, B., Joseph, K., Kunchithapautham, K., Bandyopadhyay, M., O'Quinn, E.C., Nowling, T., and Rohrer, B. (2015). Local production of the alternative pathway component factor B is sufficient to promote laser-induced choroidal neovascularization. Invest. Ophthalmol. Vis. Sci. *56*, 1850–1863.

60. Schnabolk, G., Stauffer, K., O'Quinn, E., Coughlin, B., Kunchithapautham, K., and Rohrer, B. (2014). A comparative analysis of C57BL/6J and 6N substrains; chemokine/cytokine expression and susceptibility to laser-induced choroidal neovascularization. Exp. Eye Res. *129*, 18–23.

61. Coughlin, B., Schnabolk, G., Joseph, K., Raikwar, H., Kunchithapautham, K., Johnson, K., Moore, K., Wang, Y., and Rohrer, B. (2016). Connecting the innate and adaptive immune responses in mouse choroidal neovascularization via the anaphylatoxin C5a and γδT-cells. Sci. Rep. *6*, 23794.

62. Giani, A., Thanos, A., Roh, M.I., Connolly, E., Trichonas, G., Kim, I., Gragoudas, E., Vavvas, D., and Miller, J.W. (2011). In vivo evaluation of laser-induced choroidal neovascularization using spectral-domain optical coherence tomography. Invest. Ophthalmol. Vis. Sci. *52*, 3880–3887.

63. Lohr, H.R., Kuntchithapautham, K., Sharma, A.K., and Rohrer, B. (2006). Multiple, parallel cellular suicide mechanisms participate in photoreceptor cell death. Exp. Eye Res. *83*, 380–389.

OMTM, Volume *9*

Supplemental Information

Delivery of CR2-fH Using AAV Vector Therapy as Treatment Strategy in the Mouse Model of Choroidal Neovascularization

Gloriane Schnabolk, Nathaniel Parsons, Elisabeth Obert, Balasubramaniam Annamalai, Cecile Nasarre, Stephen Tomlinson, Alfred S. Lewin, and Bärbel Rohrer

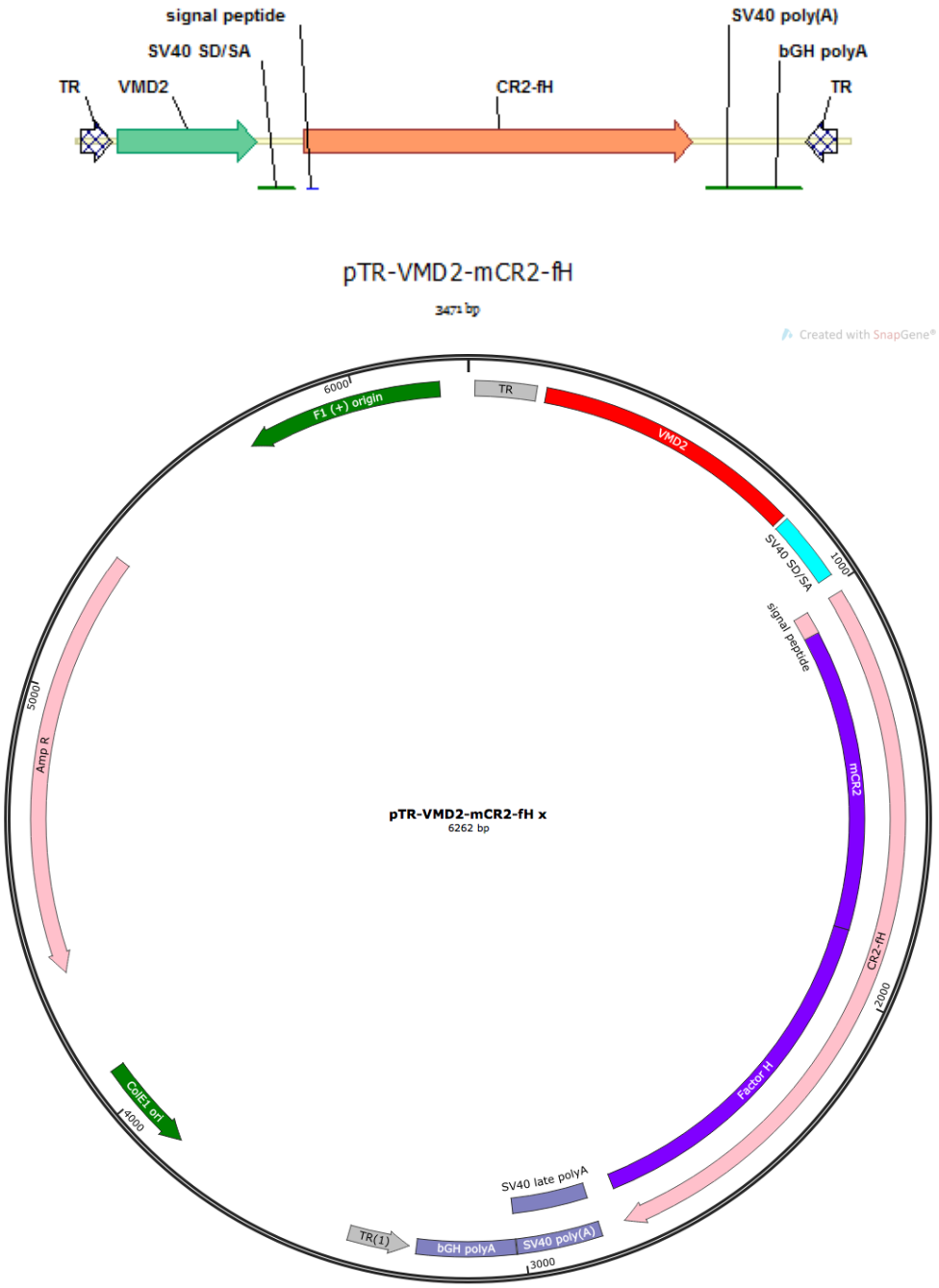

Fig S1. Map of the AAV5-VMD2-CR2-fH Vector. The AAV vector contained AAV2 terminal repeats (TR). Expression of the CR2-fH fusion protein was directed by 624 nucleotide fragment of the human *VMD2* (*BEST1*) promoter[1]. The primary transcript contained a synthetic intron (SD/SA) derived from SV40 and polyadenylation signals derived from SV40 and the bovine growth hormone (bGH) gene. The CR2-fH fusion gene consisted of 19 codons from the N-terminus of human CD1, serving as a secretion signal, 740 nucleotides derived from murine CR2 and 908 nucleotides of murine factor H. All components were confirmed by dideoxynucleotide sequencing before packaging in AA5 capsids.

1. Esumi, N, Oshima, Y, Li, Y, Campochiaro, PA, and Zack, DJ (2004). Analysis of the VMD2 promoter and implication of E-box binding factors in its regulation. *J Biol Chem* **279**: 19064-19073.